Moshe Nazarathy and Alex Tolmachev

Subbanded DSP Architectures Based on Underdecimated Filter Banks for Coherent OFDM Receivers

[<AU: please supply short subtitle as per magazine style>]

Subbanded digital signal processing (DSP) **<AU: please check that DSP is correctly spelled out>** with underdecimated (Udeci) filter banks (FBs), is a recent DSP technique whereby the optical channel bandwidth is digitally sliced into multiple spectrally disjoint subbands (SBs) to be processed in parallel. In terms of DSP hardware architecture, digital subbanding amounts to an alternative mode of parallelizing the receiver signal processing task to multiple slower processors, whereby the parallelization performed in the frequency domain (FD) rather than in the time domain (TD). We show that FD parallelization is especially suited to the long-haul optical fiber channel and present novel receiver DSP structures based on Udeci FBs, providing substantial complexity savings for ultra-high-speed optically coherent transmission.

Digital Object Identifier 10.1109/MSP.2013.2291015
Date of publication: XXXXX

INTRODUCTION

FBs have been known in DSP for decades and applied to electrical wireless and wireline communication [1]. Oversampled FBs [2], more recently referred to as *Udeci FBs* [3], form an FB subclass enjoying several advantages over critically decimated (Cdeci) or critically sampled FBs. We show that digital subbanding based on Udeci FBs may provide sizable savings of complexity in the DSP section of coherent optical receivers (Rx) **<AU: please note that the use of italics for emphasis is not permitted as per magazine style. However, italics used to introduce new terms, as preceded by "referred to" or "termed" is and italics are kept>** over ultra-high-speed fiber-optic links, as well as improve spectral efficiency and performance.

Udeci FBs are likely to become a key enabling technology for multi-Tb/s optical receivers, as they help improve the energy efficiency of the multi-Tb/s networks as the data throughput continues to grow.

<AU: Please note that text summarizing article has been removed as per magazine style. Also, Table 1 was removed

since all definitions are given in text: Table 2 was then renumbered to Table 1 and relevant table citations fixed in text>

OVERVIEW OF RECENT OPTICAL DETECTION TECHNIQUES AND THEIR USE OF DSP TECHNIQUES

We briefly review recent trends in photonic transmission, exploring commonalities and differences versus electrical communication techniques, motivating the role of FB DSP techniques in the upcoming generation of optical communication systems for multi-Tb/s transmission.

OPTICALLY COHERENT DETECTIPON

In recent years, we have witnessed the advent and commercial deployment of optically coherent detection (OCD) [4], whereby a laser is used in the Rx as an optical local oscillator (OLO), in addition to having a laser in the transmitter (Tx) as an optical source. The coherent optical Rx demodulates the received optical field, mixing it with the OLO field via the quadratic detection effect provided by the photodiodes (PDs). If the LO frequency does not coincide with that of the signal, then the net result is the downconversion of the optical spectrum to an IF electrical frequency, providing the front end of a coherent optical heterodyne receiver. Having the two frequencies (nearly) coincide and using two OLOs in quadrature results in homodyne (or intradyne) coherent detection, generating the IQ **<AU: can IQ be spelled out?>** components of the optical field complex envelope (CE) (or equivalently magnitude and phase) Subsequently, analog to digital conversions followed by DSP may be applied in the optical receiver. OCD is a recent trend, rapidly making its way into large-scale commercial deployment. In contrast, earlier optical communication techniques had been traditionally based on optical direct detection (ODD), essentially using the Rx PD as a power detector. The ODD quadratic detection generates the squared magnitude of the optical field, erasing field phase information. Gaining access to the full CE by means of OCD is a "game changer," motivating advanced DSP in the Rx.

THE AGE OF DSP IN OPTICALLY COHERENT TRANSMISSION

Once optical field CE becomes observable by means of OCD, there should be, in principle, little difference between modern electrical wireless or wireline Rx-s versus coherent optical Rx-s. Photonic OCD is just as an extremely wideband case of detection of ultra-high rate data modulated onto an extremely high-frequency carrier. This point of view has spurred within the optical communication community a trend of porting to OCD a host of detection structures and DSP techniques originally developed in the context of electrical transmission. Optical communication researchers have been competing in identifying various modulation formats and DSP techniques to be adopted for advantageous OCD use.

DISTINGUISHING TRAITS OF PHOTONIC TRANSMISSION

Nevertheless, the long-haul fiber-optic channel bears unique traits, differing from electrical wireless/wireline media in five major respects.

1) The fiber-optic channel is ultra-broadband, enabling long-haul fiber links for data and voice communications backbones of national or global coverage. Over the broadband optical spectrum, wavelength division multiplexing (WDM) techniques are used to densely frequency-multiplex multiple optical channels, each of which typically occupies several tens of GHz and carries data rates the order of 100 GB/s. An optical channel is typically two to three orders of magnitude faster than what is customary in electrical transmission, making DSP design and application-specific integrated circuit (ASIC) realization of the optically coherent Rx extremely challenging. Here we address for definiteness the Rx DSP for a single optical channel, with typical bandwidth (BW) of 25 GHz, transmitting quadrature phase shift keying (QPSK) or 16-QAM (BW refers in this article to the full spectral support of a signal, not 3 dB BW). Ultra-dense wavelength division multiplexing (WDM) of multiple such channels to form Tb/s optical superchannels, is treated elsewhere in this issue of *IEEE Signal Processing Magazine*.

2) Third-order nonlinear effects unique to the fiber-optic propagation (in contrast, wireless/wireline electrical channels are typically linear). This article focuses on linear processing—nonlinear impairment mitigation is addressed elsewhere in this issue.

3) Extremely long delay spread (duration of the channel impulse response) of long-haul fiber links due to the accumulation of chromatic dispersion (CD) for the wideband signals. As CD is a linear effect, it may be mitigated by linear equalizer (EQZ) filters. Note that dispersive delay spread is also present in wireline transmission, e.g., over telephony DSL and electrical power lines. However, the channel memory of long-haul fiber-optic links is on the order of 100 symbols, which is one to two orders of magnitude longer than in electrical transmission. This indicates that the CD EQZ requires an excessive number of taps, even if optimized by using an FD EQZ such as overlap save (OLS). Notice that for second-order dispersion multiple CD EQZ filter taps are characterized by a single degree of freedom, specifically the CD differential group delay parameter (higher-order CD would entail additional degrees of freedom.

4) The single-mode fiber (SMF)-optic channel is inherently 2×2 multiple input, multiple output (MIMO), as it supports two orthogonal polarizations (POL), referred to here as X- and Y- POL. The polarization mode dispersion (PMD) effect implies that the fiber dispersive delay spread is POL-dependent. PMD is impacted by environmental fiber disturbances on a sub-ms scale, hence it must be adaptively tracked by the 2×2 MIMO equalizer (moreover, the EQZ taps must be tunable to absorb the uncertainty in the estimation of the amount of CD). Granted, MIMO techniques of even higher dimension have proliferated in wireless transmission.

Nevertheless, at ultra-high symbol rate, the 2×2 MIMO EQZ with $4 \times O(10)$ taps memory takes its toll onto the overall complexity of coherent Rx DSP.

5) The acceptable outage probabilities in the high-capacity long-haul optical trunks are several orders of magnitude lower than in typical wireless links, impacting the selection of DSP algorithms, e.g., to mitigate outage effects due to PMD.

COHERENT Rx COMPLEXITY

It turns out that in a typical modern coherent Rx, operating at tens of GS/s, the two linear EQZ functions—CD EQZ and POL/PMD 2×2 MIMO EQZ—dominate the Rx DSP computational complexity (reflected mainly in the number of multipliers), and place excessive requirements on area and power consumption of ASIC implementations of the DSP section of the Rx. As transmission rates are expected to follow a Moore-like growth law, the Rx DSP complexity is identified as a bottleneck about to stifle the expansion of the Internet backbone infrastructure. Minimizing DSP computational load without sacrificing performance is recognized as a critical goal of the modern photonic receiver algorithmic system design. We aim to show that known FB DSP techniques may be applied along with novel extensions to advance the complexity reduction/energy-efficiency objective, contributing to the continued growth of the global communications.

MULTICARRIER TECHNIQUES IN OPTICAL COMMUNICATIONS

Multicarrier techniques such as OFDM are widespread in electrical transmission and have made their way into optical communication as well [5]–[9], though not yet commercially deployed. Intense research and debate continues on the relative merits of single-carrier (Nyquist) versus multicarrier (OFDM) formats for optical transmission [10], [11]. Figure 1 presents the block diagram of a state-of-the-art conventional coherent optical OFDM Rx for a single optical channel. In fact, the shown system is augmented to incorporate the so-called DFT-spread (DFT-S) variant (also adopted in fourth-generation wireless transmission under the revised name single-carrier FDMA, but still dubbed DFT-S in optical communication [7]). Note that in wireless transmission, this technique is used in a multiple access context, whereas in photonic long-haul transmission it is proposed to be used to transmit multiple tributaries point-to-point. In DFT-S [7], in addition to the main MN-pnt OFDM FFTs in the Rx (one for each polarization), an array of M (I) FFTs each of size N are used in the Tx and the Rx to effectively generate and detect M parallel tributaries, which may be viewed as frequency multiplexed narrower band single carrier signals (SCs). Advantages of DFT-spread OFDM include reduced peak-to-average power ratio and improved nonlinear [12] and phase noise tolerances.

BRIEF HISTORICAL ACCOUNT OF DIGITAL FBs FOR OCD

Actually, FBs are routinely used in optical communication without naming them as such. In particular, the WDM optical channelization technique, essentially assembling/separating out multiple transmissions at different "colors" (wavelengths/optical frequencies), may be viewed as an analog form of FB, albeit in the optical domain. However, our interest is in digital FBs.

In 2009, Ho [13] was the first to propose a coherent optical link based on Udeci (oversampled) FBs, pointing out a

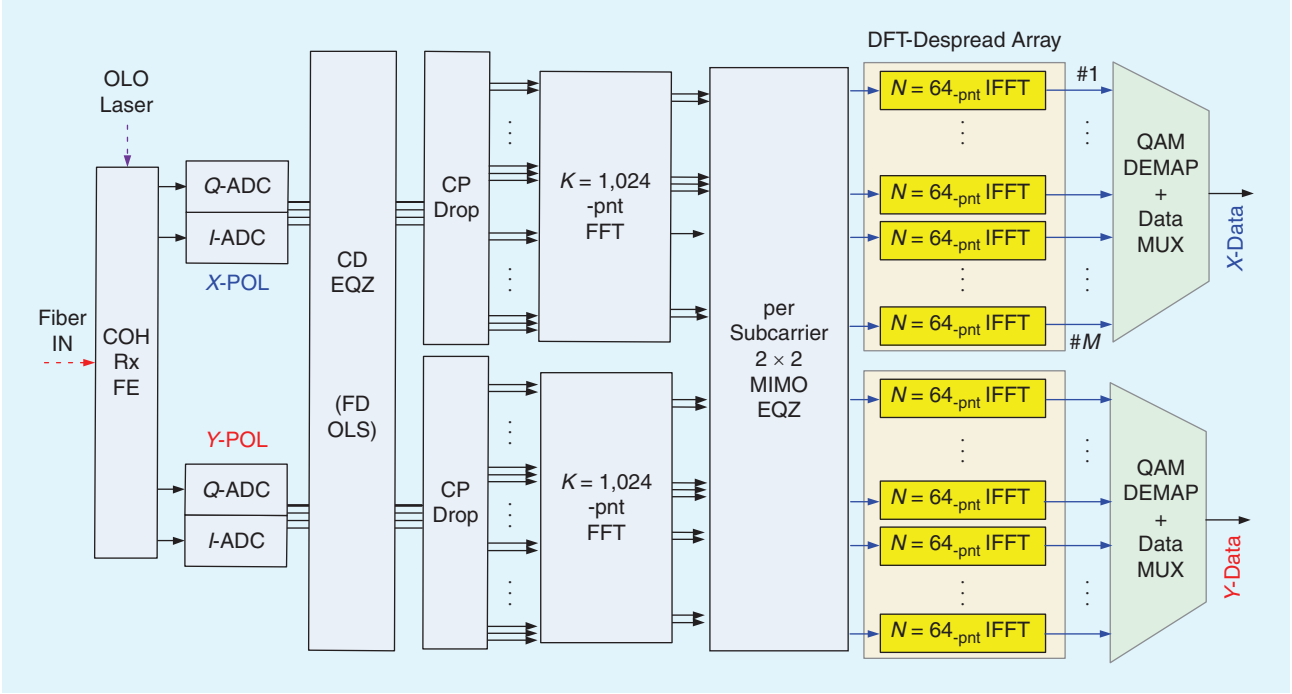

[FIG1] The conventional high-speed DFT-S OFDM Rx, where FE stands for front end and CP for cyclic prefix. The OFDM Tx is not shown but it is essentially the DSP dual of the Tx, comprising two IFFTs, one for each POL. A plain OFDM Rx (non-DFT-S) may be obtained by simply removing the DFT-despread array.

substantial complexity advantage upon performing the CD EQZ on an SB basis. He observed that Udeci FBs may be potentially realized with lower complexity than a Cdeci FB, for a given channel BW and number of SBs and for comparable distortion, but did not elaborate on specific DSP structures realizing such advantage.

CD EQUALIZATION ADVANTAGE OF SUBBANDED Rx

Here we reinterpret Ho's argument regarding the CD EQZ complexity reduction, expanding and quantifying it as follows: Let $C[\mu]$ measure the complexity cost (e.g., the multipliers count) of the CD EQZ, with $\mu = \lceil \Delta\tau T_s^{-1} \rceil$ the CD delay spread gauged in units of discrete-time sampling intervals, T_s. For an FIR TD implementation of the EQZ, $C = O(\mu)$, whereas for an FD implementation, $C = O(\log \mu)$ (the log stemming from the Cooley–Tukey DFT fast algorithm). In turn, the analog delay spread is $\Delta\tau = \beta_2 L \cdot B$, where L is the fiber length and β_2 is the CD parameter. The sampling rate also varies proportionally to the BW, $T_s^{-1} = \eta B$ (with η a factor related to the spectral efficiency and oversampling ratio). The CD delay spread is then $\mu = \lceil \beta_2 \eta L \cdot B^2 \rceil$, quadratic in the BW. The impact of slicing the total channel BW, B, into M SBs (B/M per SB) and using a separate CD EQZ in each SB is dramatic—the delay spread in each SB is reduced by a factor of M^2. For an FIR TD EQZ, the complexity per SB is reduced by a factor of $O(M^2)$, whereas for an overlap-save FDE EQZ the complexity per SB is reduced by a factor of $O(M \log M)$. Since there are M SBs operating in parallel, the total CD EQZ complexity is M times larger and the savings and the final CD EQZ savings are $O(M)$ for a TD EQZ and $O(\log M)$ for an FD EQZ. For example, for a $B = 25$ GHz channel transmitted over a 2,000 km link of standard SMF, $\mu = 150$ taps, slashed down to $\mu/M^2 = 150/15^2 = 2/3$ for $M = 15$ SBs, i.e., a fraction of a single tap per SB. Thus, just a single tap EQZ suffices to fix the CD in each SB, as further elaborated in the section "Subband Processors–2×2 MIMO DFT-S OFDM Receivers." Once the channel spectrum has been sliced into multiple SBs, the SB processors become extremely simple. This is an instance of a divide and conquer algorithm, with the divide performed in the FB and the conquer occurring in the multiple SB Rx-s, the complexity of all of which together is much lower than the complexity of a full-band Rx—provided the FB realization overhead is kept sufficiently low (in the section "Novel Efficient Realization of a $2\times$Udeci FB Core by Combining a Pair of Cdeci FBs," we show how to efficiently implement the Udeci FB).

Fast-forwarding to 2013, Liu et al. [14] experimentally demonstrated this concept by long-haul optical transmission over a subbanded system constructed on the basis of a DFT-spread OFDM structure acting as an equivalent FB, realized by inserting appropriate spectral guardbands within each SB. Their offline SW verified that the CD EQZ becomes more computationally efficient when the number of SBs is increased. Further improvements are desired to reduce the spectral overhead used for the guardbands that incurred about 10% spectral efficiency loss, and to increase in the number of SBs to enjoy even higher subbanding complexity advantage. This spectral efficiency challenge is addressed in our own Udeci FB approach, but prior to that, let us mention that the subbanding concept surfaced in the last few years in the coherent optical OFDM context. Du and Lowery [15] proposed an OFDM-based subbanding technique at the Tx-side, without addressing its complexity of realization. An optical OFDM review by Jansen [5] accounted for the subbanding advantage in OFDM transmission in terms of a reduction in the cyclic prefix (CP) duration, which may be taken as the CD delay spread per SB, hence should vary as $(1/M)\Delta\tau = (1/M)\beta_2 L \cdot B$, substantially reduced for large SB count, M. However, Jansen assumed that the slicing into SBs is optically performed, by means of numerous narrow band optical channels, each with its DAC, optical modulator at the Tx, optical channel filter, coherent optical front-end, analog-to-digital converter (ADC), DSP ASIC at the Rx, which would be highly inefficient in HW resources as well as inefficient in spectral efficiency due to the required optical guardbands. Evidently, the digital subbanding approach based on FBs would be preferable, provided the digital complexity could be reduced in both the FB core and in the SB processors, which act as mini-Rx-s in their own right albeit over narrowband SBs. We made our contribution to this objective [16]–[23] by introducing efficient implementations of Udeci FBs and dechannelizers for (DFT-S) OFDM Rx-s. We have been inspired in our own approach mostly by harris [3], [24], [25] (note that this author insists on spelling his name in lowercase) but our approach has evolved beyond it in several respects, as we focus on OFDM. For the Udeci FB core itself, we present an alternative different realization equivalent to harris'. Their DSP Rx structures, constructed around their Udeci FB core realization, are not equivalent to ours but typically have a different focus—intertwining data modulation with up/down frequency conversion and multiple sampling rate conversions. This is a distinct perspective than ours—we rather devote the Udeci FB to the specific DFT-S OFDM context, utilizing it for the "divide" part of "divide and conquer." The harris Udeci FB structure differs from our novel structure yet incurs the same multipliers count, however, it might be less suitable for high-speed optical communication, as it is less amenable to time-parallelization due to its state-machine structure of the cyclic buffers at the I/O of the polyphase filter array. A harris dechannelizer would be more costly to implement in an ultra-high-speed ASIC as required for optical communication. In contrast, our Udeci FB realization is much simpler, "recycling" two well-known Cdeci FB modules, interconnecting them to form a Udeci FB (see the section "Novel Efficient Realization of a $2\times$ Udeci FB Core by Combining a Pair of Cdeci FBs"). HW **<AU: please spell out HW; should this be "hardware?">** designers would appreciate this realization simplicity.

In the HW efficiency area, we make a contribution to both the Udeci FB core and the rest of the Rx, by combining the generic Udeci FB core with additional DSP (interpolators/decimators) to generate a complete multichannel (de)channelizer. The resulting scheme may be interpreted as a DFT-Spread OFDM receiver (DFT-S features PAPR and phase noise advantages versus plain

[TABLE 1] SOME OPERATORS OF MULTIRATE THEORY—OUR NOTATION.

${}^{v}O_{u}^{(\text{param})}$	GENERIC OPERATOR	${}^{v}O_{u}\{x[u]\} = y[v]$	LABELED BY I/O VARIABLES AND PARAMETERS
IDFT^{M} DFT^{M}	(INVERSE) DFT	$X[\beta] = {}^{\beta}\text{IDFT}_{p}^{M-\text{pnt}}\{x[p]\} = \sum_{p=0}^{M} x[p]\bar{W}^{p\beta}$ $x[p] = {}^{p}\text{DFT}_{\beta}^{M-\text{pnt}}\{X[\beta]\} = (1/\text{M})\sum_{p=0}^{M} X[\beta]\bar{W}^{-\beta p}$	$\bar{W}_M = e^{j2\pi/M}$; $W_M = e^{-j2\pi/M}$
$[x]_R$	MODULO-R REDUCTION	$[x]_R \equiv x \bmod R \Leftrightarrow x = \lfloor x/R \rfloor R + [x]_R$ $[\bullet]_R: \mathbb{R} \mapsto [\nu_0, \nu_0 + R),\ R, \nu_0 \in \mathbb{R}$ or $[\bullet]_R: \mathbb{Z} \mapsto \{k_0, k_0 + 1, \ldots k_0 + R - 1\},\ R, k_0 \in \mathbb{Z}$	DEFINED FOR EITHER REALS OR INTEGERS FOR REALS, TYPICALLY $\nu_0 = 0$ OR $\nu_0 = -R/2$
$C^{[s]_R}$	CIRCULAR SHIFT MODULO-R	$C_{\nu}^{[s]_R}\{X(\nu)\} \equiv X([\nu - s]_R)$	s IS THE DELAY PARAMETER
$\downarrow L$	DOWNSAMPLING	$\{x[k]\}_{\downarrow L} \equiv x[kL],\quad L \in \mathbb{Z}$	
$\uparrow L$	UPSAMPLING	$\{y[k]\}_{\uparrow L} \equiv \{\ldots, \underbrace{y[0], 0, 0, \ldots, 0}_{L}, \underbrace{y[1], 0, 0, \ldots, 0}_{L}, \ldots\}$	
$x_{p}^{[p]^{type}}[k]$	pTH-POLYPHASE COMPONENT MODULO-P (TYPE $\in \{1, 2, 3\}$) OF A SEQUENCE $\{x[k]\}$	$x^{[p]_p^{\prime}}[k] \equiv x[kP + p] = \{x[k + p]\}_{\downarrow P}$ $x^{[p]_p^{\prime\prime}}[k] \equiv x[kP + (P - 1 - p)]$ $x^{[p]_p^{\prime\prime\prime}}[k] \equiv x[kP - p] = \{x[k - p]\}_{\downarrow P}$	FOR TYPE-1 BY DEFAULT, WE DISCARD THE TYPE SUPER, SCRIPT: $x^{[p]_p}[k] \equiv x^{[p]_p^{\prime}}[k]$
$S/P^{(1:L)}$	1:L SERIAL-TO-PARALLEL MODULE	$S/P^{(1:L)}$: $x[k] \rightarrow \left\{x^{[0]_L^{\prime\prime\prime}}[k], x^{[1]_L^{\prime\prime\prime}}[k], \ldots, x^{[L-1]_L^{\prime\prime\prime}}[k]\right\}$	GENERATES THE TYPE-3 POLYPHASE COMPONENTS

OFDM). To our knowledge, we are the first to disclose OFDM Rx structures based on Udeci FBs. In contrast, in [26], multichannel techniques based on Cdeci FBs for electrical communication were considered as an alternative to OFDM. In our approach we do not pit the filter bank versus OFDM techniques against each other as mutually exclusive options, but we combine them to advantage in efficient OFDM receiver structures based on Udeci FBs rather than Cdeci FBs.

Our most recent contribution is to "go experimental" [23], but not in an offline optical transmission experiment (optically propagated signals acquired by ultra-fast samplings scopes and processed offline, which gains the title "experimental" in optical communication) but rather we prepare for the fastest ever "online" experiment. We have recently constructed and tested a real-time FPGA at the unprecedented 25 Gbaud (Gsamp/s) symbol rate for DFT-spread OFDM with 16-QAM modulation. This is work in progress, with back-to-back electrical fiber transmission already demonstrated over the real-time field-programmable gate array (FPGA) incorporating all Rx processing functions, but optical transmission is not shown yet. Electrically, our Rx was shown to process 160 Gb/s over the 25-GHz optical channel BW over dual polarizations and was able to inspect any SB.

In the last two years, other contributions to digital subbanding by FBs have been made by Randel et al. [27], [28], focusing on spectrally efficient real-time implementation at the Tx side, using multicarrier offset-QAM. This complements our own FB-based work on real-time Rx-s [23].

A recent work on digital subbanding from Huawei and related academics [29] has reinvented elements of our previously published approach, bringing CD equalization down to a single tap along with integer delay per SB, duplicating a concept from our previous proposal and simulations [16]–[19], [21], [22], which we recently demonstrated in FPGA HW [23].

Cdeci VERSUS Udeci UNIFORM FBs

As the Udeci FBs are DSP structures, we must be precise in our development of these concepts, so we are now "going mathematical" aided by the operator notation listed in Table 1.

An FB is defined as a collection of filters with common input or output. In a communication link based on FBs (Figure 2), at the Tx we place a synthesis FB (S-FB), forming the Tx output as the sum of the outputs of S-FB filters, in turn fed by M tributary signals to be "multiplexed" for transmission. The tributary signals may undergo some preprocessing at the tributary level. At the Rx, a corresponding Analysis FB (A-FB) acts as a demultiplexer. The received signal is 1:M split to feed a collection of filters. After some optional postprocessing, the filter outputs (M outputs of the A-FB) should ideally reconstruct the tributary signals launched at the Tx-side.

We are interested in uniform FBs, meaning that filters forming the FB are all band-pass filters (BPFs) with spectral passbands appearing identical around their center frequencies, which are on a regular grid along the frequency axis, ν, at S [Hz] separation. The total frequency span for the whole FB is $R = MS$. In our case, R coincides with the optical channel BW (and with the inter-channel frequency spacing in a WDM multichannel system). The FB slices the channel spectral support into M SBs with $S = R/M$ spectral separation). The uniform FB requirement is equivalent to having all BPFs transfer functions (TFs) consist of uniformly shifted replicas of a prototype filter (PF) TF: $H_{\beta}(e^{j2\pi\nu/R}) = H_0(e^{j2\pi(\nu - \beta S)/R})$. Equivalently the impulses responses (IRs) $h_{\beta}[k] = Z^{-1}\{H_{\beta}(z)\}$ (with Z the z-transform) are harmonic modulations of the IR, $h_0[k]$, of the PF: $h_{\beta}[k] = e^{j2\pi\beta k/M} h_0[k] = \bar{W}_M^{\beta} h_{\beta}[k]$.

As BW is reduced by a factor of M upon going from the channel down to the SB level, it is useful to downsample the BPF outputs by some integer factor, L. In particular, for $L = M$, we have a classic FB structure, referred to as *critically*

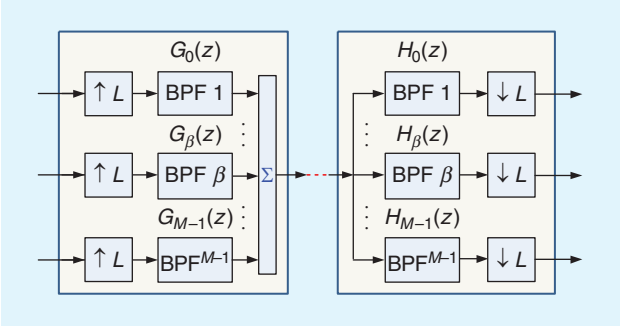

[FIG2] Back-to-back synthesis and analysis FBs, Cdeci ($L = M$), and underdecimated ($L < M$).

sampled or *critically underdecimated*. This Cdeci FB has been known for half a century. In this case, if the PF is designed with one-sided BW S, then each SB is sampled at its Nyquist rate, $S = R/M$. If $L < M$, the FB is referred to as oversampled or underdecimated. (e.g., [3], [24], and [25]) In such Udeci FB, the SBs are oversampled by a factor of $V = M/L > 1$, referred to here as the *Udeci-factor*; the corresponding Udeci FB is referred to as $V\times$ Udeci. This article treats twice-underdecimated ($2\times$ Udeci) FBs ($V = 2$, $L = M/2$), but for generality, some derivations will be carried out for arbitrary V, setting $V = 2$ at the end.

We commence with the Cdeci class case ($V = 1$), specifically Figure 2 with $L = M$, reviewing its well-known polyphase realization, referred to as *uniform DFT* (*U-DFT*) *FB*. This efficient Cdeci FB realization is not allocated a separate figure here, as it is taught in most DSP textbooks, e.g., [25], but its specification is as follows: a 1:M serial-to-parallel (S/P) module feeding an array of M polyphase filters, the outputs of which in turn feed an M-pnt DFT. The polyphase filters have IRs $\{h_0^{[\gamma]_M}\}_{\gamma=0}^{M-1}$, given by the M polyphase components of the PF filter $h_0[k]$ (see Table 1 for polyphase components definition). The classic U-DFT realization of the Cdeci FB (shown as the submodule marked Cdeci #1 or #2 in Figure 3) is far more efficient than a brute-force approach of M BPFs in parallel (Figure 2), nevertheless it not efficient enough, since the requisite number of taps of the PF (equal to the sum of the number of taps of the polyphase filters) is still prohibitive. The reason for having too many taps is that the BPFs forming the A-FB, used to carve the channel into spectrally disjoint SBs, must have nearly rectangular TFs, to prevent either crosstalk between SBs or loss of spectral efficiency. Such nearly brick-wall PF typically require $O(10^3)$ taps. This hampers the applicability of classic Cdeci FBs to energy-efficient communication applications such as optical transmission, motivating the adoption of Udeci FBs. However, the U-DFT Cdeci FB will emerge as a building block in our novel efficient implementation of the Udeci FB.

NOVEL EFFICIENT REALIZATION OF A 2 × Udeci FB CORE BY COMBINING A PAIR OF Cdeci FBs

Udeci FB structures are obtained by setting $L = M/V < M$, or equivalently $V > 1$ in Figure 2 (in particular, $V = 2$ for $2\times$ Udeci FBs). These FBs are inefficient in the form of Figure 1, as

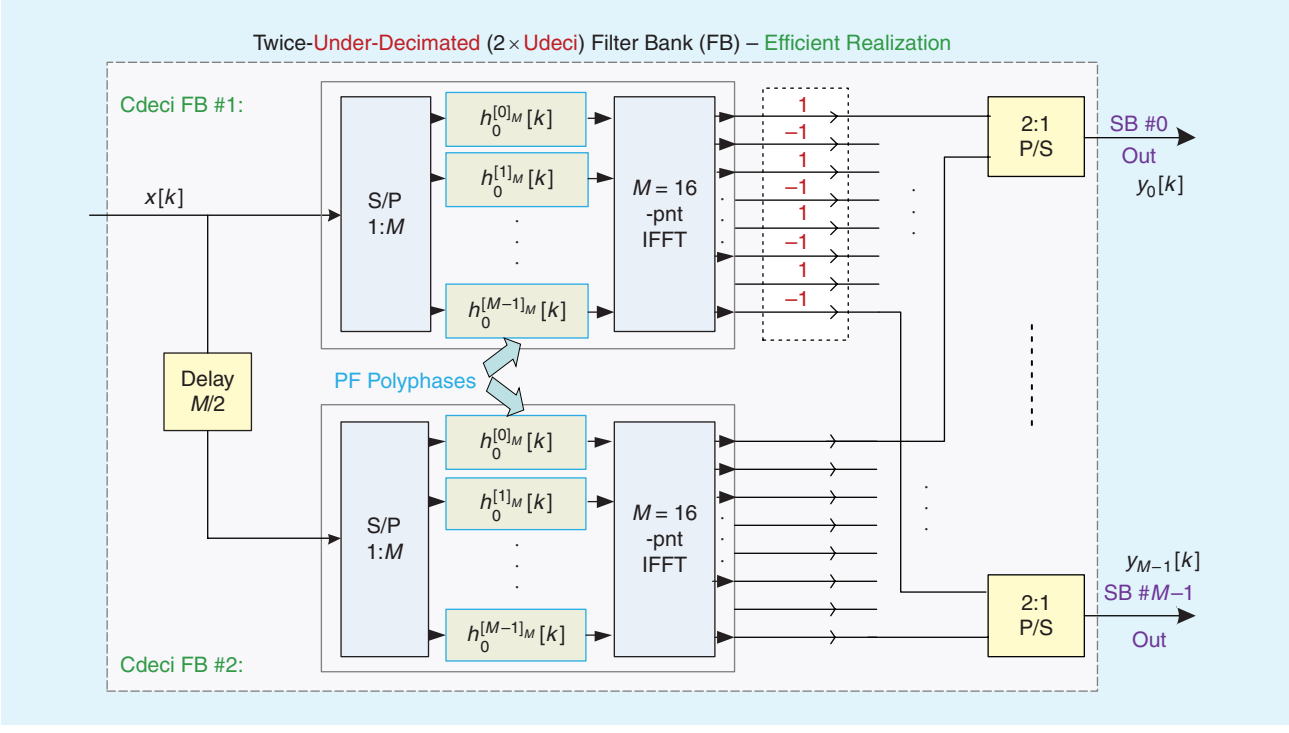

[FIG3] Novel efficient structured $2\times$ Udeci FB realization based on interleaving a pair of Cdeci FBs. The M outputs of Cdeci FB#1 are alternated in sign and time-interleaved with the corresponding M outputs of Cdeci FB#2 yielding for each of the M output SB signals at rate $2R/M$ where R is the rate of $x[k]$.

the realization of multiple sharp BPFs at high speed is very complex. Here we disclose for the first time an efficient polyphase realization of a uniform $2\times$ Udeci FB, conveniently structured as interconnection of a pair of U-DFT Cdeci FB modules (Figure 3), making it easy to implement the FB in HW (or in SW **<AU: please spell out SW>** at much lower speeds) as the Cdeci FB, to replicated twice to make a Udeci, is a well-known module for which HW cores already exist (one major FPGA maker supplies a Cdeci FB core).

The "glue" connecting the two Cdeci modules to form a $2\times$ Udeci A-FB is very simple, as shown in Figure 3. One Cdeci FB input is delayed by $L = M/2$, whereas the outputs of the other Cdeci FB are alternated in sign (modulated by ±1). Equivalently, in case we have access to the internals of the Cdeci FB, we may replace the ±1 alternation by a half-wave circular shift, swapping of the upper and lower halves of the input vector into the DFT, statically crossing the wires.

The two Cdeci FB modules provide the even and odd components of the outputs $y_\beta[k]_{\beta=1}^{M}$ of the $2\times$ Udeci A-FB, thus if we require the FB output in serial form, we just interleave the two M-pnt output vectors generated by the two Cdeci FBs, by means of $M/2$ 1:2 Parallel/Serial (P/S) modules. Our proof that Figure 3 is equivalent to the generic A-FB structure at the Rx side of Figure 2 (with L there taken as $M/2$) is based on first deriving the polyphase modulo L IRs, $\{h_\beta^{[\gamma]_L}[k]\}_{\gamma=1}^{L}$, for each of the $M = 2L$ BPFs of the $2\times$ Udeci FB, in terms of the L polyphases $\{h_0^{[\gamma]_L}[k]\}$ of the PF

$$h_\beta^{[\gamma]_L}[k] = h_0^{[\gamma]_L}[k](-1)^{\beta k}\tilde{W}_{2L}^{\beta\gamma}, \qquad \beta = 0,1,\ldots,2L-1; \quad \gamma = 0,1,\ldots,2L-1. \tag{1}$$

A polyphase representation of the output of any filter followed by $\downarrow L$ downsampling is derived in most DSP textbooks based on Noble's identities (e.g., [25]), and is applied here to express the βth output of the Udeci FB, in response to the wideband input $x[k]$ into the FB

$$y_\beta[k] = \sum_{\gamma=0}^{L-1} x^{[\gamma]_L^{III}}[k] \otimes h_\beta^{[\gamma]_L}[k]. \tag{2}$$

Interestingly, the type-3 polyphases of the input signal interact with the type-1 polyphases of same order of the filter IR. Eq. **<AU: please clarify what "Eq." stands for here. Is this referring to a particular equation number?>** fully specifies the I/O mapping of the 2xUdeci FB (which is a 1:2L SIMO system), but its direct realization would not be most efficient. It remains to manipulate this equation (with Eq. **<AU: please clarify what Eq. stands for here: is this a particular equation number?>** set in) to bring it to a form equivalent to the highly efficient form of Figure 3. The derivation is omitted but it is based on Table 1 and multirate properties.

Let us compare our resulting efficient Udeci FB realization of Figure 3 with prior ones by harris et al. [3], [24], [25], and also by our group (our current novel realization differs from our prior realization **<AU: edit OK?>** introduced in [18], which was based on $M/2$ single-input, dual output (SIDO) polyphase filters preceding the M-pnt DFT). It turns out that all three Udeci FB realizations incur the same multipliers count, however our two alternative realizations (in [18] and here) feature a high-speed operational advantage over that of harris', due to easier time-parallelization, as explained in the section "Brief Historical Account of Digital FBs for OCD."

(DE)CHANNELIZER BASED ON Udeci FBs PLUS INTERPOLATORS/DECIMATORS

In our recent optical communication-oriented research [16]–[23], we presented DSP structures augmenting the Udeci FBs at the Tx and Rx by additional elements, converting them to multichannel (de)muxes, or (de)channelizers with nearly perfect reconstruction (Figures 4–5). The added elements are interpolators/decimators, combined with the efficient Udeci core of the last section to form a complete distributed (de) channelizer system. At the Tx-side, by attaching V-fold interpolators on the input ports of the S-FB at the Tx, we obtain an FD-mux of multiple input tributaries; at the Rx-side, by attaching V-fold interpolators on the input ports of the A-FB, we obtain a dechannelizer or FD-demux of the transmitted tributaries. Circular shifts are further inserted between the interpolators/decimators and the FB ports to perform frequency up/down conversions.

The resulting (de)channelizers feature four advantages: 1) low HW complexity, 2) the SB are extracted flat and sharp (brickwall-like filtering per SB, nearly perfect reconstruction), 3) no spectral guardbands required between SBs, and 4) the SBs retain orthogonality.

Using our dechannelizers, channel impairments may be equalized on an SB basis. Unlike in FB structures with perfect reconstruction [2], our nearly perfect reconstruction is not based on mutual cancellation of spectral crosstalk among neighboring SBs (which would be impaired by the distortion generated by the transmission channel).

As opposed to [3], our approach is to keep the (de)channelization and per-SB processing functions well separated. Any subsequent processing per SB is to be performed in separate array of SB processors attached to each of the SBs (not shown in Figure 4).

Our principle of operation is that the filtering be partitioned into two tiers:

- coarse prefiltering at the FB level within each of the constituent BPFs is no longer required to be brickwall, but is now relaxed to have mild frequency responses (Figure 6), shaped akin to trapezoids rather than rectangles, flat over the SB extent, S, with mild transitions spanning neighboring S intervals
- sharp pre- and postfiltering in the interpolators/decimators, efficiently realized in the FD by back-to-back (I)FFTs of different sizes, as further explained.

This structure provides (de)channelization at reduced overall computational load relative to a Cdeci FB. Indeed, the extra complexity of the interpolators/decimators (which operate at slower rate) turns out to be just a fraction the complexity

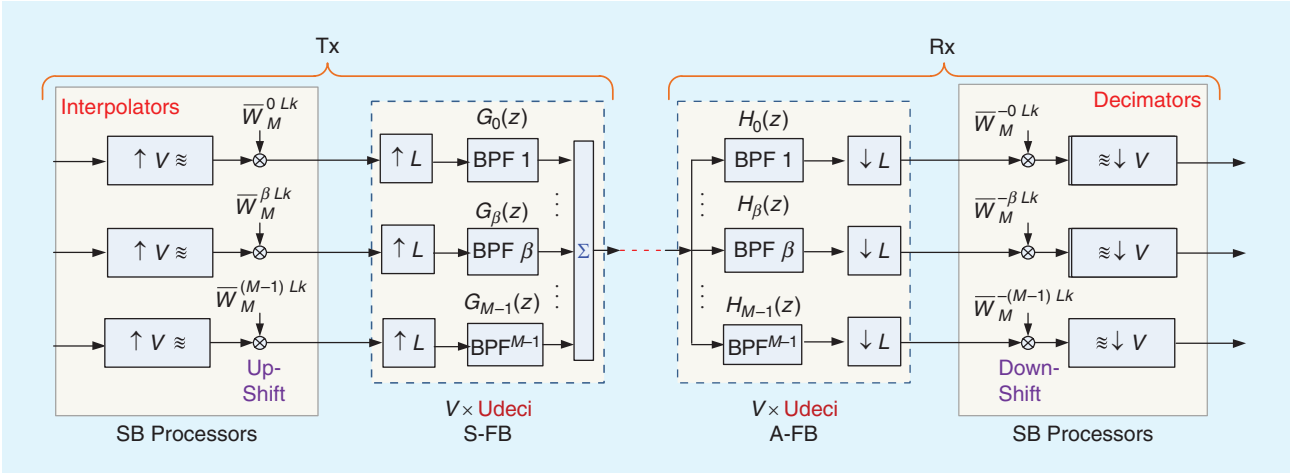

[FIG4] The (de)channelizer with no spectral overhead and with nearly perfect reconstruction. The interpolators and decimators comprise up/downsampling followed/preceded by brickwall low-pass filtering performing image rejection/antialiasing, respectively.

reduction gained by replacing the sharp brickwall filters of a Cdeci FB, requiring lots of taps, by milder-sloping filters of the Udeci FB, requiring far fewer taps.

At this point, let us invoke DSP-duality to heretofore exclusively treat Rx-side A-FB structures, as the Tx-side S-FB structure is the DSP-dual of the A-FB, with all signal flows running in reverse. Moreover, as shown in the next section, the S-FB at the Tx is not really necessary but may be replaced by a conventional DFT-S OFDM Tx. Thus, from now on our focus is A-FBs at the Rx.

The structure of Figure 4 is next transformed into the equivalent one of Figure 5, essentially realizing the V-fold decimators in the FD as cascades of an N-pnt DFT a circular shift and a VN-pnt IDFT (and its dual at the Tx). The equivalence is due to decimation amounting to band-limiting low-pass filter (LPF) followed by downsampling. The LPF is performed in the cyclic FD, discarding DFT frequency samples corresponding to the blocked band at the IDFT input. The modulations (frequency up/down shifters) appearing in Figure 4 are realized by the FD circular shifts in Figure 5.

It is useful to analyze the (de)channelizer scheme of Figure 5 (specialized to $V = 2$) in the spectral domain, as depicted in Figure 6. The mild trapezoidal filter, H_β, nearly perfectly passes through over its flat-band the βth SB, along with residual interference from the two neighboring SBs. The figure illustrates how the $L = M/2$-fold decimation generates L spectral images, aliasing the filtered signal all the way down to baseband, where a nearly perfect image of the desired SB is carved out by the twofold decimator. This figure applies to the case of an even SB index, β. In the case of an odd SB index, a similar analysis (not illustrated) would indicate that the twofold decimator should be preceded by a half-band circular shift, essentially picking up the upper (high-pass) spectral half of the downsampled output of the odd-indexed BPF.

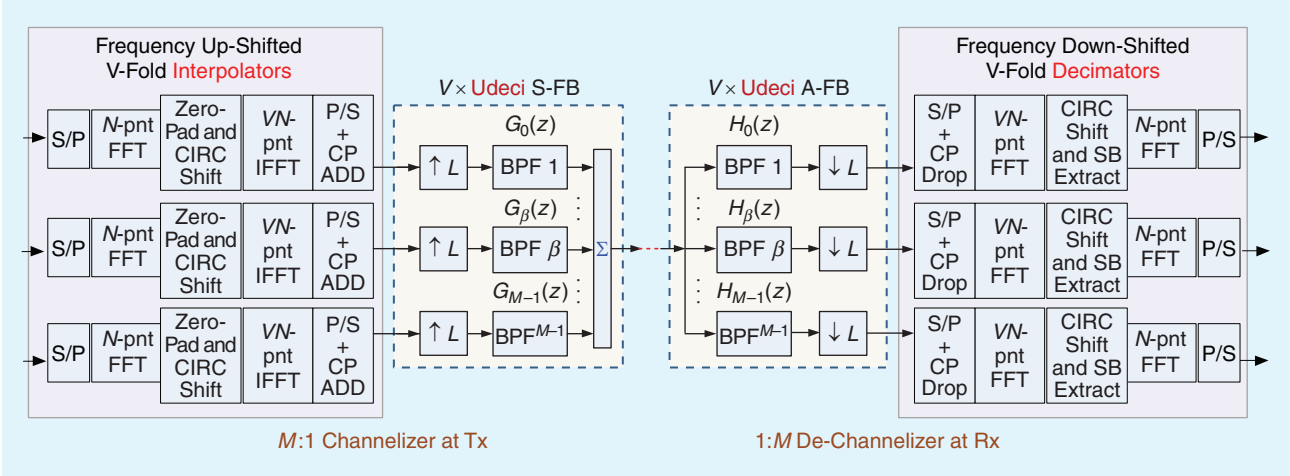

[FIG 5] The Tx-side channelizer and Rx-side dechannelizer with nearly perfect reconstruction based on efficient (I)FFT-based realization of the interpolators/decimators in the (de)channelizer of Figure 4.

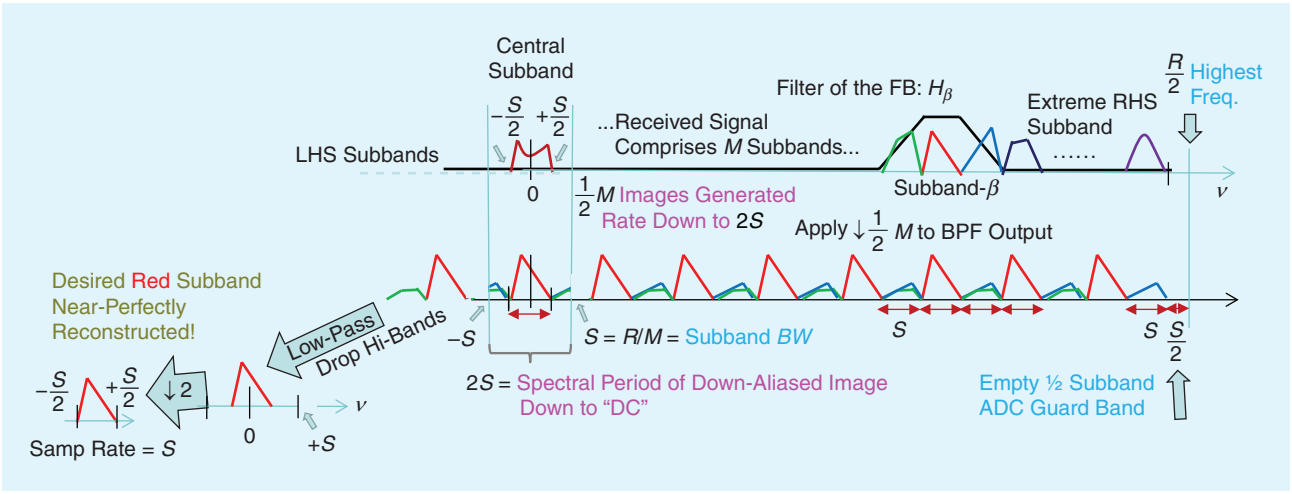

[FIG 6] Spectral analysis of the Rx-side dechannelizer in Figure 5 (for an even SB index, β). The mild trapesoidal-like filter of the FB selects the desired SB along with remnants of the adjacent SBs. The downconversion effect generated by (M/2)-fold downsampling brings down to baseband the desired SB along with interference from the two neighbors. The final low-pass filtering action of the decimator singles out the desired SB.

THE 2 × UDECI FB BASED DECHANNELIZER APPLIED TO (DFT-S) OFDM TRANSMISSION

In Figure 5 we presented an FB-based (de)channelizer, at the Tx and Rx respectively. To transmit an OFDM channel, multiple mini-OFDM tributaries may be launched within each SB. In this case, the Rx side may be simplified (Figure 7). Once multiple SB OFDM Rx-s are added at A-FB outputs in Figure 5 to detect the OFDM tributaries, the N-pnt IFFTs within these SB OFDM Rx-s end up stacked back-to-back with the N-pnt FFTs of the decimators of Figure 5, and mutually cancel out. Thus, for OFDM tributaries, the overall subbanded Rx may be realized as in Figure 7.

Moreover, it turns out that the Tx-side channelizer is not necessary for OFDM– it may be replaced by a conventional OFDM Tx as shown in Figure 8, wherein each SB carries a subset of OFDM tones—a "mini-OFDM" signal in itself. The overall OFDM spectrum, as generated by a conventional OFDM Tx, essentially an IFFT, may be conceptually viewed as composed of a juxtaposition of contiguous SBs filled up with "mini-OFDM" signals. Nevertheless, the same logic is not extensible to the Rx-side—the OFDM FFT is not equivalent to an A-FB. Indeed, the dispersive delay (CD) over the fiber channel causes OFDM symbols in different SBs to arrive at Rx at different times. The Rx (RHS in Figure 8) must slice the SBs by means of "true" linear filtering (rather than cyclic filtering as realizable in the DFT domain), by means of an FB followed by an array of SB Rx-s, essentially realizing the structure of Figure 7. The OFDM Rx structure of Figure 8, with an efficient Udeci FB, implements a divide and conquer strategy, performing the "divide" (slicing into SBs) by means of the 2 × Udeci A-FB while the "conquer" is performed in the multiple SB Rx-s, each processing a SB, with reduced BW S, a factor of M lower than the BW R of the full optical channel. The SB Rx-s become extremely simple, even M of them together are more than two times simpler than a full-band Rx. For example, if R = 25 GHz is the channel BW, then for M = 16 SBs we require 16 SB Rx-s—actually 15, as the 16th SB, the outer one, split into two halves at the two extreme ends of the channel, is used as transition region for the ADC—without incurring any spectral efficiency penalty provided the technique of orthogonal band multiplexing (OBM) [8] is used.

(DFT-S) OFDM RECEIVER BASED IN 2 × UDECI FBS—TOP VIEW

The description above pertained to OFDM over a scalar channel. For coherent optical OFDM, each digitally subbanded Rx must

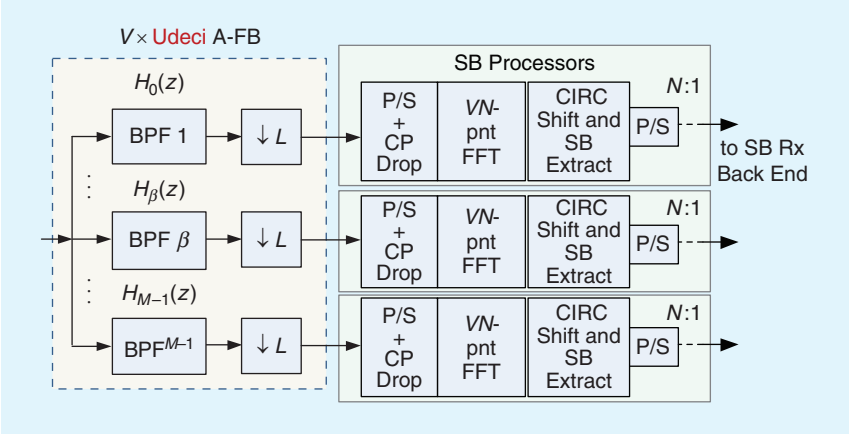

[FIG 7] Novel FB-based OFDM Rx obtained by placing onto the output ports of Figure 5 N-pnt IFFTs (associated with the OFDM Rx tributaries) and canceling them out versus the N-pnt FFTs of the decimators. The V-fold Udeci A-FB is efficiently realized as in Figure 3.

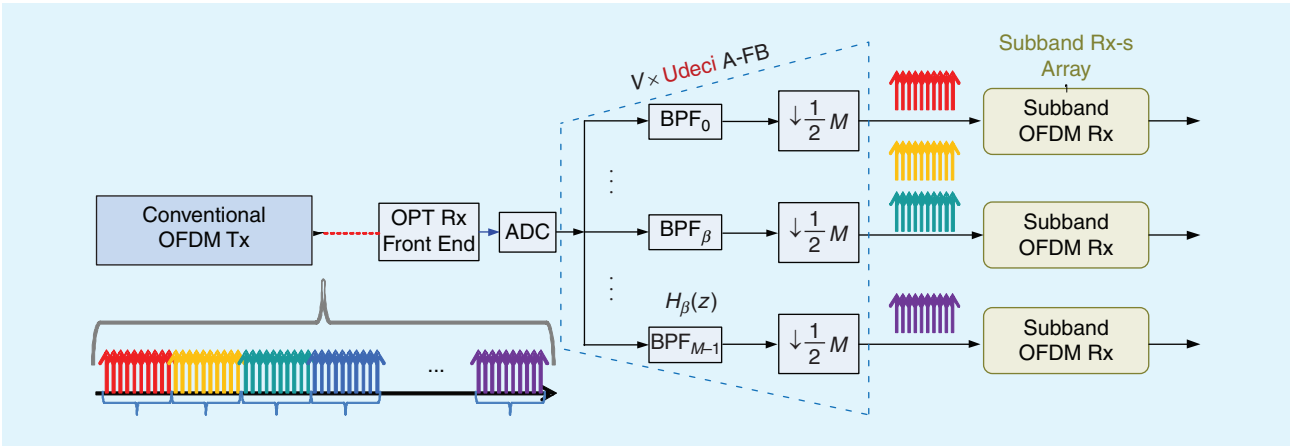

[FIG8] The OFDM link using a conventional OFDM Tx. The Rx essentially comprises a 2×Udeci FB followed by an array of SB OFDM Rx-s. The *MN*-tones OFDM symbol generated by the Tx may be conceptually viewed as the spectral juxtaposition of *M* OFDM symbols, each containing *N* tones, each associated with an SB. The analysis FB in the Rx separates out the individual "mini-OFDM" signals and presents them to *M* SB OFDM Rx-s, each one of which processes one SB.

contend with two orthogonal POLs, therefore the top level of the overall Rx (Figure 9) is equipped with a pair of 2xUdeci FBs, slicing out the the X- and Y-POL signals into SBs, sent in pairs to the SB processors, which are actually 2×2 MIMO OFDM Rx-s (the βth SB outputs of X- and Y-FBs are routed to the βth SB Rx, with β indexing the M output ports of the two FBs).

SUBBAND PROCESSORS–2×2 MIMO DFT-S OFDM RECEIVERS

Figure 10 "zooms" into one of the SB Rx-s, presenting its internals. This is a MIMO OFDM Rx, relaxed to detect an M-times narrower spectral band (S=R/M=25 GHz/15=1.66 GHz rather than 25 GHz in our system, which is substantial relief, despite the multiplicity of 15 such Rx-s). Due to the 2xUdeci nature of the FB, each SB Rx is twice-oversampled at sampling rate $2S$=3.33 GHz.

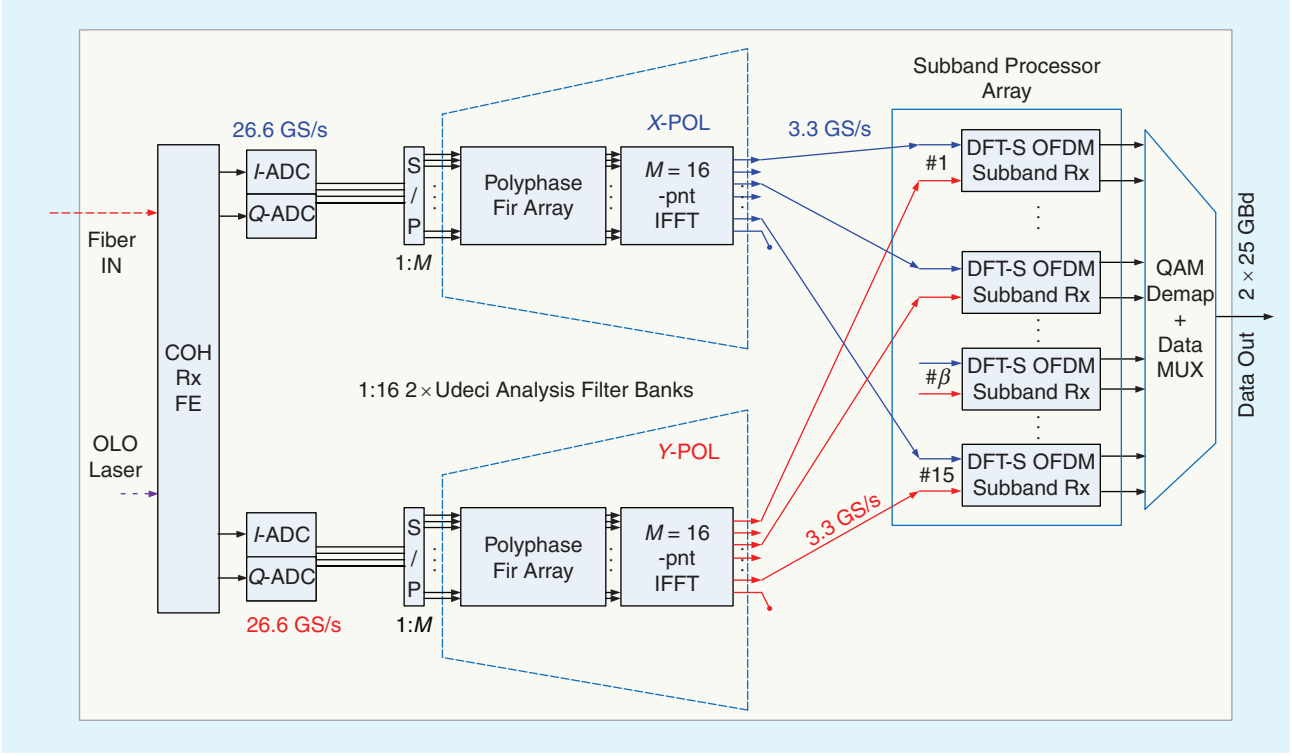

[FIG 9] Subbanded (DFT-S) OFDM Rx. The top level shows the two FBs for the X- and Y-polarizations and the array of SB Rx-s. Notice that each SB Rx is fed by the corresponding SBs from the two $2 \times$ Udeci FBs associated with the two POLs.

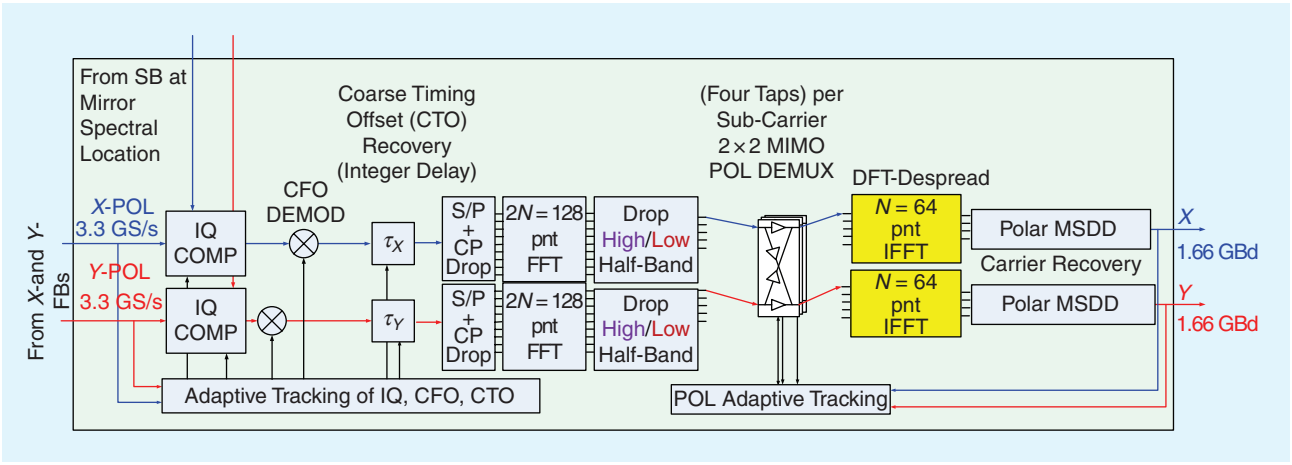

[FIG 10] The detail of each of the SB Rx-s in Figure 9 <AU: Edit ok?>. This 2 × 2 MIMO DFT-S OFDM Rx contains a full suite of DSP algorithm for signal conditioning, albeit at M/2 = 8 times reduced rate, relative to the full channel BW+ADC oversampling guardband.

The backbone of the SB Rx is the 2*N*-FFT and the *N*-IFFT, forming (for *V*=2) the *V*-fold decimator of Figure 5, completing dechannelization with nearly perfect reconstruction, in conjunction with the preceding A-FB cores shown in Figure 9. The extra DSP functions incorporated in the SB Rx-s are IQ imbalance and carrier frequency offset (CFO) mitigation, coarse (integer) and fine (fractional) timing recovery, joint CD+ POL EQZ (2 × 2 MIMO) and carrier phase recovery (CPR). The SB Rx features multiple innovations in these individual DSP modules. In particular 1) a recently introduced polar variant [30] of the multisymbol delay detection (MSDD) CPR with low complexity eliminating all multipliers, 2) in each SB Rx, the CD and POL-demux EQZ is jointly performed with just four taps, whereas in a conventional receiver there would be a full OLS FD EQZ required to mitigate CD, as well as 4 x O(10) taps to mitigate POL rotation and PMD. This underscores the substantial complexity advantage of our FB-based Rx versus a conventional full-band one, and 3) robust IQ imbalance correction scheme acting on SBs in pairs.

TOTAL Rx COMPLEXITY

The total complexity savings for 4,000-km transmission over standard SMF is 57%, as itemized in Figure 11 (*complexity* is defined here as multipliers count in the FPGA). At 2,000 km, also for a MIMO memory duration of 12 samples for a conventional full-band system, the subbanded savings would be 54.5%. Lower savings (16.6% at 2,000 km and 26.5% at 4,000 km) would be obtained if the MIMO equalization were to be incorporated within the OLS frequency-domain equalizer, however this option is still under investigation in the literature, pending a satisfactory solution to training the coefficients of such equalizer.

The key rationale for per-SB timing recovery and channel (CD and POL) EQZ is that each SB is practically frequency-flat—the quadratic phase profile of the CD over frequency appears like a sloped straight segment over the narrowband *S*=1.66 GHz BW of each SB—a linear phase slope means a constant delay per SB (regularly increasing from each SB to the adjacent one). The integer part of the SB delay (measured in SB samples units) may be readily corrected by a FIFO **<AU: please spell out FIFO>** buffer, whereas the fractional part of the delay and any other residual distortion of the almost frequency-flat SB may be corrected by a single complex tap EQZ. This

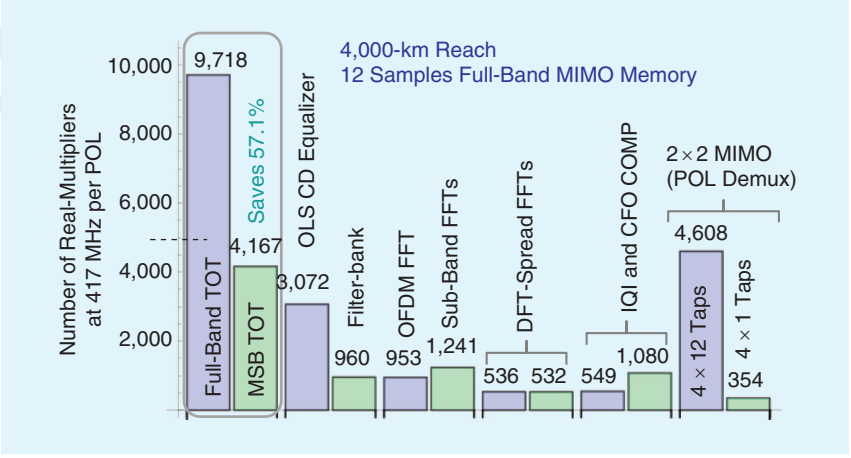

[FIG 11] The complexity comparison of a full-band conventional Rx versus a multisubband (MSB) DFT-S OFDM Rx for 4,000-km transmission over SMF and for 12 taps of memory for the conventional POL-demux 2 × 2 MIMO equalizer. Most MSB savings stem from more efficient CD and 2 × 2 MIMO (PolDemux) EQZ. The 2xUdeci FB "overhead," which enables these savings, is seen to be just several percent of total Rx complexity. Both systems designed to target the same high spectral efficiency over 2,000-km SSMF: Very low CP spectral overhead of 1.56% = 2/128 = 8/1,024. Full-band DFT-S OFDM Tx (used with both Rx-s) uses 1,024-pnt OFDM symbol and inserts eight samples of CP MSB subband Rx-s <AU: is sentence missing punctuation? Should comma be added? Sentence is unclear, please clarify> simply drop one CP sample every 128 samples. Full-band Rx needs heavy CD and adaptive 2 × 2 MIMO equalizers in the TD, before the OFDM.

indicates a substantial advantage in CD equalization complexity for an SB receiver. For an OFDM Rx, the timing recovery function is much simplified relative to a single-carrier Rx, as delay and correlate (D&C) algorithms such as Schmidl–Cox are degraded by CD. Here, the frequency-flat SBs yield improved D&C performance per SB. Moreover, the quite complex parallelization of D&C algorithms [31] is now simplified. The net result is more robust and simpler timing recovery. More generally, in a full-band Rx, control path functions such as channel estimation and adaptive tracking generally take a major toll on complexity and performance. In contrast, the digitally subbanded Rx does not require separate CD estimation and enjoys substantial advantage in all its adaptive algorithms, which converge much faster and more accurately over each frequency-flat SB. The underlying reasons for adaptive advantage are 1) the taps count per SB is very small (typically two per POL) and 2) the eigenvalue spread of the autocorrelation matrix of the received signal is very small here. It is well known in adaptive filtering theory that the eigenvalue spread of matrix controls the speed of convergence of an adaptive filter and that increased frequency ripple or variation of the signal power spectral density is indicative of increased eigenvalue spread. Thus, convergence of adaptive filters in each SB is generally much faster than convergence of an adaptive filter operating in each SB." **<AU; is this a quote? Please clarify if opening quotation marks are needed and provide source of quote>** Rapid and accurate adaptive algorithms convergence means low data-aided overhead: the training sequences launched in each SB may be taken shorter. **<AU: "may be taken shorter" is unclear, kindly clarify if possible>**

REAL-TIME HW IMPLEMENTATION OF A 16-QAM DFT-S OFDM RX

The complexity savings and treelike nature of the FB $\rightarrow$ SB array enabled our setting a record in the real-time FPGA realization of a DFT-S OFDM Rx, albeit fed at this point not by actual ADCs, but from synthetic 16-QAM simulated data played out from a FIFO at full-speed (25 Gbaud / POL x 2 POL, carrying an aggregate 160 Gb/s going through the FB). We used two ML628 boards and layouts of the two XC6HX380T Virtex6 FPGAs, one for the FB and the other for the SB Rx. For now we just implemented a single FB but a full 2×2 MIMO SB Rx out of the $M = 15$ ones (feeding one POL input of the SB Rx from data passing in real time through the FB, whereas the data on the other path is simulated offline, establishing the real-time functionality of both the FB and the MIMO OFDM SB Rx. For demo purposes, a single SB Rx may be used to access and detect any of the 15 SBs of the full 25-GHz optical channel, one at a time (each SB carries $(1/15)\,160$ Gb/s $= 10.66$ Gb/s). Note that the limitation in accessing all SBs at once is neither of algorithmic DSP nature, nor due to computational inefficiency, but it is rather extraneous—inter-FPGA interconnectivity bottlenecks, which would be irrelevant in actual ASIC implementation **<AU: please check that edited sentence retains original meaning>**. This validates real-time feasibility of our FB-based 2×25 Gbaud 16-QAM Rx.

DISCUSSION AND CONCLUSIONS

We aimed to establish that FB-based digital subbanding is a preferred architecture for high-speed ASICs for optical communication. The subbanding scheme is not analog, but it is rather purely digital, performed after A/D conversion for each individual channel in the WDM multiplex, amounting to a second tier of fine frequency division demultiplexing. Digital subbanding provides benefits similar to those obtained by multiband OFDM techniques [7]–[9]. In those techniques, relatively narrowband bands (3–6 GHz) are photonically generated within a superchannel structure, multiplexed at the Tx and demultiplexed at the Rx, an approach recently increasingly adopted in superhero OFDM superchannel experiments, e.g., [6]. In contrast, our digital subchannel demux requires much simpler, lower-cost, and energy-efficient hardware. As our subbanding realization is digital rather than analog, we do away with the cumbersome finely spaced multitone generator, and we eliminate a large number of DACs, ADCs, modulators, optical filters, and analog optical receivers, which would be customarily used in transmission of a finely spaced (3–6 GHz) analog-generated superchannel. Nevertheless, we enjoy the full benefits of having narrowband frequency-flat SBs, which are now digitally (de)muxed. Furthermore, despite efficiently crowding the multiple 1.6 GHz SBs with zero spectral guardbands, we are nevertheless able to maintain a nearly perfect degree of orthogonality between the individual SBs (i.e., eliminate inter-SB crosstalk), which would have been impossible in a fine-muxed analog/optical-generated superchannel. Finally, by OBM [8] at the OFDM WDM channel level (in our exemplary system between neighboring 25-GHz channels) we are able to further eliminate the interchannel guardbands among the WDM bands.

Another aspect pertains to the effectiveness of the current Udeci subbanded approach to detection of SC modulation. For SC coherent receivers, CD, timing, polarization, frequency offset, and other impairments may also be best compensated per SB basis. The analysis FB and the array of SB receivers must be complemented by a synthesis FB or equivalent means assembling the final SC signal out of the individually processed SBs. Such SC subbanded architecture turns out to be more effective than conventional single-carrier structures, however, this topic is deferred to a future publication.

The FB-based receivers presented here were developed in the photonic context but may also be found useful for wireline and wireless electrical transmission.

REFERENCES

[1] P. Vaidyanathan, "Filter banks in digital communications," *IEE Circuits Syst. Mag.*, vol. 1, no. 2, pp. 4–25, 2001.

[2] Z. Cvetkovic and M. Vetterli, "Oversampled filter banks," *IEEE Trans. Signal Processing*, vol. 46, no. 5, pp. 1245–1255, May 1998.

[3] M. Awan, Y. Le Moullec, P. Koch, and F. Harris, "Polyphase filter banks for embedded sample rate changes in digital radio front-ends," *ZTE Commun.*, vol. 8, no. 4, pp. 3–9, 2011.

[4] X. Liu and M. Nazarathy, "Coherent, self-coherent and differential detection," in *Impact of Nonlinearities on Fiber Optic Communications*. New York: Springer, 2011, Chap. 1. **<AU: Please check the location of publisher.>**

[5] S. L. Jansen, "OFDM for optical communications," in *Proc. Optical Fiber Communication Conf.* (*OFC'10*), 2010, p. SC341.

[6] W. Shieh and I. Djordjevic, *OFDM for Optical Communications*. Amsterdam,

The Netherlands: Elsevier, 2010.

[7] Y. Tang, W. Shieh, and B. S. Krongold, "DFT-spread OFDM for fiber nonlinearity mitigation," *IEEE Photon. Technol. Lett*., vol. 22, no. 16, pp. 1250–1252, Aug. 2010.

[8] W. Shieh, Q. Yang, and Y. Ma, "107 Gb/s coherent optical OFDM transmission over 1000-km SSMF fiber using orthogonal band multiplexing," *Opt. Express*, vol. 16, no. 9, pp. 6378–6386, Apr. 2008.

[9] X. Liu and S. Chandrasekhar, "High spectral-efficiency transmission techniques for beyond 100-Gb/s systems, SPMA1," in *SPPCom—Signal Processing in Photonic Communications—OSA Techn. Dig*., 2011, pp. 1–36.

[10] S. Kilmurray, T. Fehenberger, P. Bayvel, and R. I. Killey, "Comparison of the nonlinear transmission performance of quasi-Nyquist WDM and reduced guard interval OFDM," *Opt. Express*, vol. 20, no. 4, pp. 4198–4208, 2012.

[11] R. Schmogrow, M. Winter, M. Meyer, D. Hillerkuss, S. Wolf, B. Baeuerle, B. Nebendahl, J. Meyer, M. Dreschmann, M. Huebner, C. Koos, W. Freude, and J. Leuthold, "Real-time Nyquist pulse generation beyond 100 Gbit/s and its relation to OFDM," *Opt. Express*, vol. 20, no. 1, pp. 317–337, 2012.

[12] G. Shulkind and M. Nazarathy, "An analytical study of the improved nonlinear tolerance of DFT-spread OFDM and its unitary- spread OFDM generalization," *Opt. Express*, vol. 20, no. 23, pp. 25884–25901, 2012.

[13] K.-P. Ho, "Subband equaliser for chromatic dispersion of optical fibre," *Electron. Lett*., vol. 45, no. 24, p. 1224, 2009.

[14] X. Liu, P. Winzer, C. Sethumadhavan, S. Randel, and S. Corteselli, "Multiband DFT-spread-OFDM equalizer with overlap-and-add dispersion compensation for low-overhead and low-complexity channel equalization," in *Proc. Optical Fiber Communication Conf.* (*OFC'13*), 2013, vol. 2, no. 2, p. OW3B.2.

[15] L. B. Du and A. J. Lowery, "Mitigation of dispersion penalty for short-cyclic-prefix coherent optical OFDM systems," in *Proc. European Conf. and Exhibition on Optical Communication* (*ECOC'10*), 2010, p. Tu.4.A.5.

[16] A. Tolmachev and M. Nazarathy, "Real-time-realizable filtered-multi-tone (FMT) modulation for layered-FFT Nyquist WDM spectral shaping," in *Proc. European Conf. and Exhibition on Optical Communication* (*ECOC'11*), 2011, paper We.10.P1.65.

[17] A. Tolmachev and M. Nazarathy, "Filter-bank based efficient transmission of reduced-guard-interval OFDM," *Opt. Express*, vol. 19, no. 26, pp. 370–384, 2011.

[18] A. Tolmachev and M. Nazarathy, "Low-complexity multi-band polyphase filter bank for reduced-guard-interval coherent optical OFDM," in *Proc. Signal Processing in Photonic Communications (SPPCom), Advanced Photonics OSA Conf.*, 2011, p. SPMB3.

[19] A. Tolmachev, M. Nazarathy, I. Tselniker, and I. Sigron, "Oversampled digital filter banks simplify and improve signal processing in RGI OFDM receivers," in *Proc. Optical Fiber Communication Conf.* (*OFC'12*), 2012, p. OM2H.3.

[20] M. Nazarathy and A. Tolmachev, "Digital subbanding—A signal processing architecture radically improving OFDM coherent optical receivers," in *Proc. SPPCom—Signal Processing in Photonic Communications—OSA Tech. Dig*., June 2012. **<AU: Please provide the complete page range.>**

[21] M. Nazarathy, A. Tolmachev, and S. Ben-Ezra, "Subbanding DSP for flexible optical transceivers," in *Proc. Int. Conf. Transparent Optical Networks (ICTON)*, 2012, no. 1. **<AU: Please provide the complete page range.>**

[22] M. Nazarathy and A. Tolmachev, "Filter-bank based digital subbanding ASIC architecture for coherent optical receivers," in *Proc. Photonics West 2013*, 2013, pp. 8647–17. **<AU: Please check the page range.>**

[23] A. Tolmachev, M. Orbach, M. Meltsin, R. Hilgendorf, Y. Birk, and M. Nazarathy, "Real-time FPGA implementation of efficient filter-banks for digitally subbanded coherent DFT-S OFDM receiver," in *Proc. Optical Fiber Communication Conf.* (*OFC'13*), 2013, p. OW3B.1.

[24] F. J. Harris, C. Dick, and M. Rice, "Digital receivers and transmitters using polyphase filter banks for wireless communications," *IEEE Trans. Microwave Theory Tech*., vol. 51, no. 4, pp. 1395–1412, 2003.

[25] F. J. Harris, *Multirate Signal Processing for Communication Systems*. Englewood Cliffs, NJ: Prentice Hall, 2004.

[26] B. Farhang-Boroujeny, "OFDM versus filter-bank multicarrier," *IEEE Signal Processing Mag*., vol. 92, pp. 92–112, May 2011.

[27] S. Randel, A. Sierra, X. Liu, S. Chandrasekhar, and P. Winzer, "Study of multicarrier offset-QAM for spectrally efficient coherent optical communications," in *Proc. European Conf. and Exhibition on Optical Communication* (*ECOC 2011*), p. Th.11.A.1.

[28] S. Randel, S. Corteselli, S. Chandrasekhar, A. Sierra, X. Liu, and P. J. Winzer, "Generation of 224-Gb/s multicarrier offset-QAM using a real-time transmitter," in *Proc. Optical Fiber Communication Conf*. (*OFC 2012*), vol. 30, p. OM2H.2.

[29] I. Slim, A. Mezghani, L. G. Baltar, J. Qi, F. N. Hauske, and J. A. Nossek, "Delayed single-tap frequency-domain chromatic-dispersion compensation," *Photon. Technol. Lett*., vol. 25, no. 2, pp. 167–170, 2013.

[30] A. Tolmachev, I. Tselniker, M. Meltsin, I. Sigron, and M. Nazarathy, "Efficient multiplier-free FPGA demonstration of for high performance phase recovery of 16-QAM," in *Proc. Optical Fiber Communication Conf*. (*OFC 2013*). **<AU: Please provide the complete page range.>**

[31] Q. Yang, N. Kaneda, X. Liu, S. Chen, W. Shieh, and Y. K. Chen, "Digital signal processing for multi-gigabit real-time OFDM," in *Proc. Signal Processing in Photonic Communications (SPPCom'11), Advanced Photonics OSA Conf*., 2011, vol. 1, no. c, p. SPMB2. **<AU: Please check whether the issue number is correct.>**

[SP]

CALLOUTS

UDECI FBS ARE LIKELY TO BECOME A KEY ENABLING TECHNOLOGY FOR MULTI-Tb/s OPTICAL RECEIVERS, AS THEY HELP IMPROVE THE ENERGY EFFICIENCY OF THE MULTI-Tb/s NETWORKS AS THE DATA THROUGHPUT CONTINUES TO GROW.

THE U-DFT CDECI FB WILL EMERGE AS A BUILDING BLOCK IN OUR NOVEL EFFICIENT IMPLEMENTATION OF THE UDECI FB.

FB-BASED DIGITAL SUBBANDING IS A PREFERRED ARCHITECTURE FOR HIGH-SPEED ASICs FOR OPTICAL COMMUNICATION.

THE FB-BASED RECEIVERS PRESENTED HERE WERE DEVELOPED IN THE PHOTONIC CONTEXT BUT MAY ALSO BE FOUND USEFUL FOR WIRELINE AND WIRELESS ELECTRICAL TRANSMISSION.